

Confinement-potential tuning: From nonlocal to local transport

G. Müller, D. Weiss, and K. von Klitzing

Max-Planck-Institut für Festkörperforschung, Heisenbergstrasse 1, D-7000 Stuttgart 80, Federal Republic of Germany

K. Ploog

TH Darmstadt, Hochschulstrasse 10, D-6100 Darmstadt, Federal Republic of Germany

H. Nickel, W. Schlapp, and R. Lösch

Forschungsinstitut der Deutschen Bundespost, D-6100 Darmstadt, Federal Republic of Germany

(Received 12 March 1992)

We investigate experimentally the influence of the boundary confining potential on edge channel transport in the quantum Hall regime. It is demonstrated that the steepness of the confining potential and therefore the edge channel separation is much more relevant for transport phenomena observed than “bulk” properties such as the electron mean free path. We change the edge potential by brief illumination using a light-emitting diode and study the crossover from nonlocal to local transport.

Magnetotransport experiments in high mobility two-dimensional electron gas (2DEG) systems have revealed a variety of unexpected phenomena, which are difficult to explain on the basis of the standard resistivity tensor component ρ_{xx} (local transport). The longitudinal four-point resistance R_{xx} , for example, expected to be $R_{xx} = \rho_{xx}(l/w)$ was found not to scale with the ratio of voltage probe separation l and the Hall bar width w [Fig. 1(a)].¹⁻³ The strange behavior of Shubnikov-de Haas (SdH) maxima corresponding to spin-up Landau levels (LL's), in particular, their asymmetry and their strong dependence on temperature and measuring current, is just another example of such phenomena.⁴ Also striking is the existence of a nonlocal resistance $R_{26,35}$.^{5,6} If a current is applied between contacts 2 and 6 [Fig. 1(a)] a voltage can be measured between contacts 3 and 5 ($R_{26,35} = U_{35}/I_{26}$), which are well separated from the “classical” current path. In such devices the resistivity ρ_{xx} is not an appropriate intensive (geometry-independent) parameter and suggestions for a *new resistivity* for high mobility quantum Hall conductors have been made.⁵

In this Rapid Communication we demonstrate that not only the high mobility but the shape, in particular, the steepness of the edge potential, is an essential parameter which causes local or nonlocal transport. Within the framework of one-dimensional edge channels^{7,8} the transport properties of a 2DEG in high magnetic fields are governed by skipping-orbit-like states which propagate along the sample's boundary and connect the contacts. The number of edge channels corresponds to the number of fully occupied LL's in the bulk. Within the edge channel picture, only the transmission properties of the electrons at the Fermi energy E_F need to be considered. All the channels carry the same amount of current.

Barriers in the system, for example, disordered contacts,⁹ point contacts,¹⁰ or Schottky gates,¹¹ can cause an unequal current distribution. It is surprising, that such a “nonequilibrium” population can be main-

tained over macroscopic distances^{9,11-13} due to suppression of interedge channel scattering (ICS). This is the origin of nonlocal or adiabatic transport effects; the measured voltage drops depend on the properties of the whole

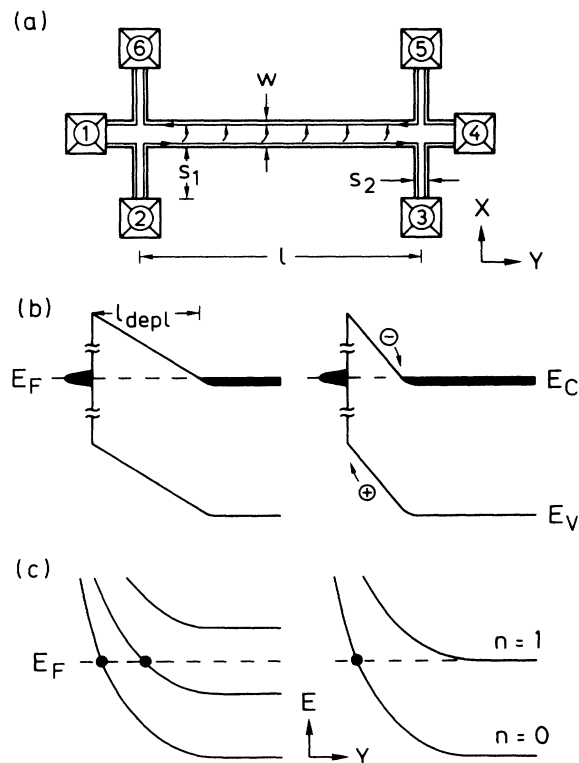


FIG. 1. (a) Schematic layout of our devices where one edge channel is sketched. Arrows hint at the backscattering process. $s_1 = 390 \mu\text{m}$, $s_2 = 50 \mu\text{m}$, $l = 0.8 \text{ mm}$, and $l/w = 8$. (b) Sketch of the lateral confining potential before (left) and after (right) illumination. (c) LL's following the edge potential with E_F between (left) and within the “bulk” LL (right).

conductor and not only on a local conductivity σ_{xx} . The equilibration length is the characteristic length describing the transition from complete adiabatic transport (absence of ICS) to equilibrated transport (equal electrochemical potentials between neighboring edge channels due to ICS). At $T = 1$ K equilibration lengths of $300 \mu\text{m}$ for scattering between spin-degenerate edge channels have been deduced.¹⁴ The equilibration length between the two spin-resolved edge channels of the lowest LL can reach values of up to 1 mm .¹⁵

If E_F is located within a bulk LL [Fig. 1(c)], backscattering from one edge to the other [sketched in Fig. 1(a)] can take place. SdH peaks emerge and the Hall resistance is no longer quantized. The SdH amplitude depends nontrivially on the coupling between the remaining edge channels and the bulk. For strong ICS, local transport behavior would be expected. If ICS is sufficiently suppressed, nonlocal phenomena as described above can be observed.

All the phenomena are understood as a consequence of a smooth lateral confining potential. Consequently, the spatial separation between neighboring edge channels ΔY becomes large; the wave-function overlap is reduced. ICS rates due to phonons and impurities are drastically reduced by a factor $\exp(-\Delta Y^2/2l_c^2)$ where $l_c = (\hbar/eB)^{1/2}$ is the magnetic length.¹⁶

Lateral patterning of GaAs-Al_xGa_{1-x}As heterojunctions with the usual etching procedures induces a lateral depletion length l_{depl} [Fig. 1(b)]. The active width of a quantum wire, for example, is significantly smaller than its geometrical width.¹⁷ E_F is assumed to be pinned in the GaAs band gap as is sketched in Fig. 1(b). For a free GaAs surface, the pinning of E_F at about midgap is well established.¹⁸ We assume that the same holds for the lateral surface of our Hall bar geometry. Illumination changes the lateral confining potential. By exciting electron hole pairs in the vicinity of the boundary, the depletion length is reduced [Fig. 1(b), right]. Holes drift

towards the edge and recombine with electrons trapped in surface states. The reduction of the l_{depl} after illumination has been verified experimentally in quantum wires¹⁷ and antidots.¹⁹ Since E_F is still assumed to be pinned at the same energetic position, the slope of the confining potential has to become steeper [Fig. 1(b)]. In the following experiment we systematically tune the shape of the edge potential using a sequence of short light-emitting diode (LED) light pulses.

Figure 1(a) shows a schematic layout of our devices patterned from high-mobility molecular-beam epitaxy grown GaAs-Al_xGa_{1-x}As heterojunctions. The samples consist of a GaAs buffer layer ($2\text{--}4 \mu\text{m}$), an undoped Al_xGa_{1-x}As spacer layer ($300\text{--}400 \text{ \AA}$), an Si n -doped Al_xGa_{1-x}As ($300\text{--}500 \text{ \AA}$) layer, and a GaAs cap layer ($100\text{--}200 \text{ \AA}$). The mesa, which defines the boundary of the device was patterned by wet chemical etching (methanol:H₃PO₄:H₂O₂, 3:1:1). We perform four-point ac resistance measurements at temperatures between 1.3 and 4.2 K using low current ($< 1 \mu\text{A}$) and frequency levels (< 15 Hz). We average the magnetoresistance over both magnetic-field directions to exclude effects due to inhomogeneities.

In Fig. 2 we compare the longitudinal resistance $R_{14,23}$ [Fig. 2(a)] with the nonlocal resistance $R_{26,35}$ [Fig. 2(b)]. The bottom traces are taken before illumination. The curves above are taken each time after a short LED light pulse. After four pulses in total (top traces in Fig. 2) the carrier density ($N_s = 2.4 \times 10^{11} \text{ cm}^{-2}$, dark) has been increased by only 5% while the mobility has been changed from $800\,000$ to $870\,000 \text{ cm}^2/\text{Vs}$. These slight changes in mobility and carrier density are accompanied by drastic changes in the measured resistances. Before illumination (bottom trace) typical nonlocal transport phenomena are clearly visible in Figs. 2(a) and 2(b). The amplitude of the SdH oscillations does not increase monotonically with the magnetic field. The line shape of the SdH oscillations is asymmetric; the spin-up levels of the first and second

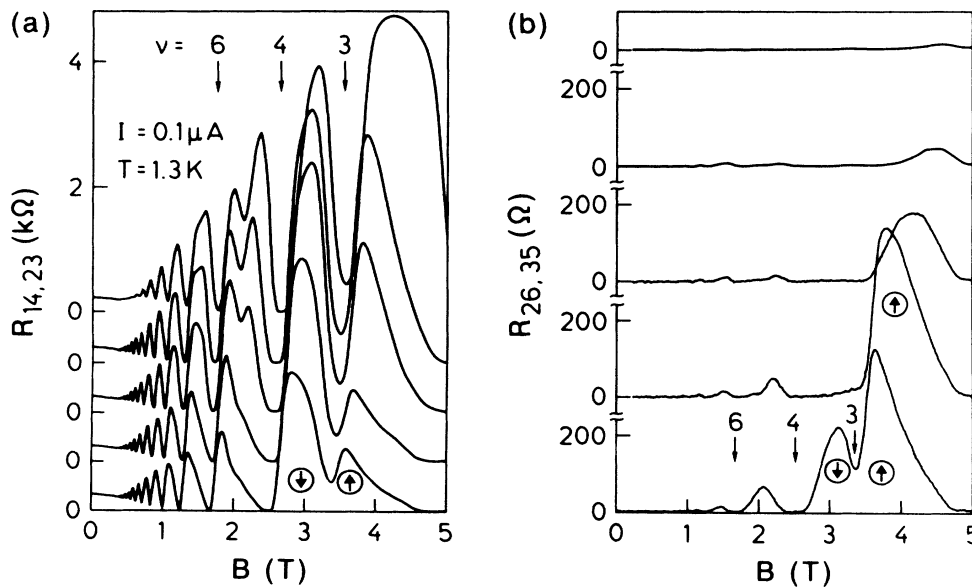


FIG. 2. (a) Longitudinal magnetoresistance before (bottom) and after several illumination steps. Arrows indicate spin orientation. (b) Nonlocal four-point resistance as function of the magnetic field under the same illumination condition as in (a).

LL ($n = 1 \uparrow$ and $n = 2 \uparrow$) are suppressed [Fig. 2(a)]. At the same B values, where deviations from the “usual” SdH oscillations emerge, large signals are observed in the nonlocal resistance $R_{26,35}$ [Fig. 2(b)].

Both effects occur in the dissipative regime where E_F is located in a spin-split bulk LL. The suppression of the SdH peak¹³ is accounted for by a decoupling between the edge channels and the uppermost (bulk) LL. The actual amplitude and shape of the SdH oscillations depend on the actual ICS rate and the conduction within the bulk uppermost LL itself. The nonlocal resistance $R_{26,35}$ is closely related to this phenomenon. A nonvanishing resistance $R_{26,35}$ requires that part of the net current, applied between contact 2 and 6, has to flow around the periphery of the device. If the ICS is sufficiently suppressed an electrochemical potential difference $\Delta\mu$ can be maintained between contacts 3 and 5 [Fig. 1(a)]. In the presence of strong ICS and backscattering $\Delta\mu$ between the upper and lower edges [see Fig. 1(a)] becomes smaller with increasing distance (in the y direction) from contacts 2 and 6. We expect a more “classical” current distribution with vanishing nonlocal resistances. The observation of such nonlocal effects in the bottom trace of Fig. 2 requires an equilibration length of the order l .

While nonlocal effects dominate the magnetoresistance *before* illumination, the situation changes drastically *after* illumination. With increasing illumination dose, the originally suppressed spin-up levels grow [Fig. 2(a)] while the nonlocal resistance maxima [Fig. 2(b)] become smaller. After the fourth LED pulse only a very weak nonlocal resistance signal can be detected [top trace in Fig. 2(b)] while fully developed SdH oscillations are observed in the longitudinal resistance [Fig. 2(a)].

After illumination the mobility is enhanced. We now face a situation where an increased mobility, usually considered as a precondition for nonlocal transport phenomena, is connected to the *suppression* of nonlocal effects.

The observed effects are consistent with our picture of illumination-induced edge potential steepening. The spatial separation ΔY between neighboring edge channels becomes smaller and ICS becomes more probable. The illumination not only reduces the edge channel separation but enhances scattering from ionized states at the etched boundary of the Hall bar. Due to the reduction of the depletion length l_{depl} the edge channels are pushed closer to the mesa boundary where those impurities are located. From our experiments we cannot distinguish between an increased ICS due to enhanced impurity scattering or due to a reduced edge channel separation.

Increasing the current level shifts the system towards equilibration due to an increased ICS rate.^{14,20} Without illumination, the same results as those shown in the top traces of Fig. 2 can be obtained if a probe current of $6 \mu\text{A}$ is used. Additional Ohmic contacts, placed on both sides of the Hall bar, also reduce the nonlocal resistance and increase spin-up SdH peaks. This gives further evidence that the effects observed after illumination originate from increased ICS.

The experiments described above have been performed in the dissipative regime where the transmission coefficients between the various contacts are not known ac-

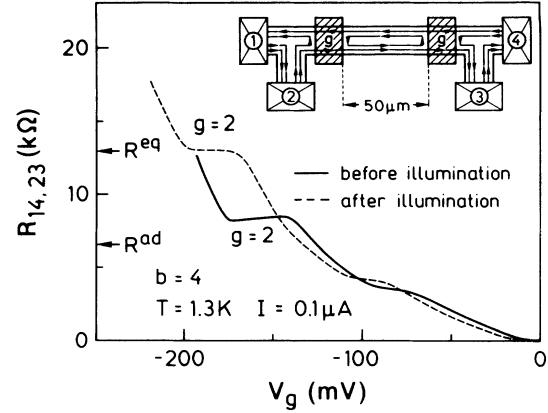


FIG. 3. $R_{14,23}$ vs gate voltage. The inset sketches the layout of the device. Hatched areas denote the Schottky gates with filling factor g underneath. b is the “bulk” filling factor. Before illumination: $N_s = 1.74 \times 10^{11} \text{ cm}^{-2}$, $\mu = 1.3 \times 10^6 \text{ cm}^2/\text{Vs}$; after illumination: $N_s = 1.95 \times 10^{11} \text{ cm}^{-2}$, $\mu = 1.7 \times 10^6 \text{ cm}^2/\text{Vs}$.

curately. A more defined situation is obtained if E_F is located between two LL’s [Fig. 1(c)], in the “bulk” of the 2DEG as well as underneath the barriers (Schottky gates). Such an arrangement¹⁵ can be used to extract the equilibration length directly from the experiment.

To investigate the magnetotransport for the integer filling factor $b = 4$, we use a geometry with two Schottky gates spaced by $50 \mu\text{m}$ (inset of Fig. 3). For complete adiabatic transport the innermost spin-degenerate edge channel circulating between the two gates decouples from the transmitted edge channel. The whole arrangement acts as a single gate and the longitudinal four-point resistance, $R_{14,23}$, is given by $R_{14,23} = h/4e^2$ (e.g., see Ref. 11). If there is strong ICS, the resistance doubles and is now the series resistance across two gates.

Figure 3 shows the longitudinal four-point resistance as a function of the gate voltage V_g , applied to both Schottky gates. Around $V_g = -170 \text{ mV}$ the outer edge channel is perfectly transmitted while the inner one is perfectly reflected (inset of Fig. 3, spin neglected). The filling factor underneath the Schottky gate is $g = 2$. Before illumination the resistance plateau is observed at $8.4 \text{ k}\Omega$, indicating adiabatic transport. An equilibration length of $160 \mu\text{m}$ for scattering between circulating and transmitted edge channel can be deduced.¹⁵ After illumination, the carrier density N_s and mobility μ are increased. Due to the increased mobility and the reduced magnetic length at $b = 4$, one would expect a reduced ICS rate and pronounced adiabatic transport. Experimentally we find the opposite.

For $g = 2$, the resistance plateau now has the equilibrated value $h/2e^2$ (within the experimental error of 3%), indicating switching from adiabatic to equilibrated transport.

The importance of the shape of the edge potential is also reflected in the observation that the adiabaticity of transport can be different after thermal cycling to room temperature even if the mobility and the carrier density are nearly identical.

In summary we have shown experiments demonstrating the transition from nonlocal to local transport by illuminating our devices. Despite an enhanced mobility adiabatic transport is destroyed. This is interpreted as a consequence of a steeper edge potential and therefore larger overlap of the edge channel wave functions. Simultaneously the edge channels come closer to the surface states at the lateral boundary, which is expected to increase the ICS rate, too. Adiabatic transport is destroyed

by steepening the edge potential for a *high-mobility* sample. We expect the opposite behavior for *low-mobility* samples (from equilibrated to adiabatic transport) if a sufficiently smooth confining potential can be imposed upon the 2DEG.

We would like to thank F. Scharfner, M. Riek, and S. Tippmann for their expert help in the processing of the samples.

- ¹K. von Klitzing, G. Ebert, N. Kleinmichel, H. Obloh, G. Dorda, and G. Weimann, in *Proceedings of the 17th International Conference on the Physics of Semiconductors, San Francisco, 1984*, edited by J. D. Chadi and W. A. Harrison (Springer, New York, 1985), p. 271.
- ²B. E. Kane, D. C. Tsui, and G. Weimann, *Phys. Rev. Lett.* **59**, 1353 (1987).
- ³R. J. Haug and K. von Klitzing, *Europhys. Lett.* **10**, 489 (1989).
- ⁴See, e.g., R. J. Haug, K. von Klitzing, and K. Ploog, *Phys. Rev. B* **35**, 5933 (1987).
- ⁵P. L. McEuen, A. Szafer, C. A. Richter, B. W. Alphenaar, J. K. Jain, A. D. Stone, R. G. Wheeler, and R. N. Sacks, *Phys. Rev. Lett.* **64**, 2062 (1990).
- ⁶K. Tsukagoshi, K. Oto, S. Takaoka, K. Murase, Y. Takagaki, K. Gamo, and S. Namba, *Solid State Commun.* **80**, 797 (1991).
- ⁷B. I. Halperin, *Phys. Rev. B* **25**, 2185 (1982).
- ⁸M. Büttiker, *Phys. Rev. B* **38**, 9375 (1988).
- ⁹S. Komiyama, H. Hirai, S. Sasa, and S. Hiyamizu, *Phys. Rev. B* **40**, 12566 (1989).
- ¹⁰B. J. van Wees, L. P. Kouwenhoven, E. M. M. Willems, C. J. P. M. Harmans, J. E. Mooij, H. van Houten, C. W. J. Beenakker, J. G. Williamson, and C. T. Foxon, *Phys. Rev. B* **43**, 12431 (1991).
- ¹¹G. Müller, D. Weiss, S. Koch, K. von Klitzing, H. Nickel, W. Schlapp, and R. Lösch, *Phys. Rev. B* **42**, 7633 (1990).
- ¹²B. W. Alphenaar, P. L. McEuen, R. G. Wheeler, and R. N. Sacks, *Phys. Rev. Lett.* **64**, 677 (1990).
- ¹³B. J. van Wees, E. M. M. Willems, L. P. Kouwenhoven, C. J. P. M. Harmans, J. G. Williamson, C. T. Foxon, and J. J. Harris, *Phys. Rev. B* **39**, 8066 (1989).
- ¹⁴S. Komiyama, H. Hirai, M. Ohsawa, H. Matsuda, and T. Fujii, in *20th International Conference on the Physics of Semiconductors*, edited by E. M. Anastassakis and J. D. Joannopoulos (World Scientific, Singapore, 1990), p. 1150.
- ¹⁵G. Müller, D. Weiss, A. V. Khaetskii, K. von Klitzing, S. Koch, H. Nickel, W. Schlapp, and R. Lösch, *Phys. Rev. B* **45**, 3932 (1992).
- ¹⁶T. Martin and S. Feng, *Phys. Rev. Lett.* **64**, 1971 (1990).
- ¹⁷T. Demel, D. Heitmann, P. Grambow, and K. Ploog, *Superlatt. Microstruct.* **9**, 285 (1991).
- ¹⁸W. E. Spicer, I. Lindau, P. Skeath, C. Y. Su, and P. Chye, *Phys. Rev. Lett.* **44**, 420 (1980).
- ¹⁹D. Weiss, M. L. Roukes, A. Menshig, P. Grambow, K. von Klitzing, and G. Weimann, *Phys. Rev. Lett.* **66**, 2790 (1991).
- ²⁰G. Müller, D. Weiss, S. Koch, K. von Klitzing, H. Nickel, W. Schlapp, and R. Lösch, in *20th International Conference on the Physics of Semiconductors* (Ref. 14), p. 829.